Local and global jamming transitions in packet transport

Kanghun Kim and B. Kahng[1]

[1]*Department of Physics and Astronomy, Seoul National University, Seoul 151-747, Korea*

(Dated: December 18, 2011)

We investigate the mechanisms underlying continuous and discontinuous jamming transitions (JTs) in packet traffic flow in the Internet, and we find that when a routing protocol causes the spreading of local congestions triggered from a few nodes to other ones, global-scale nodes become congested in a short time, and then the JT is discontinuous. Otherwise, the JT is continuous. We also find that while the system performance increases even beyond the JT point for the continuous transition, it decreases for the discontinuous transition. These differing results originate from the locality and non-locality, respectively, of congestions in the system.

PACS numbers: 64.60.aq, 89.20.-a, 89.40.-a, 89.75.Hc

Complex networks have attracted significant attention during the last decade. Many interesting properties ranging from network structure to dynamics on/of networks have been uncovered, and are still actively investigated [1–4]. Among the various kinds of complex networks, transportation networks such as the Internet have been the focus of much of this research; as the amount of digital data increases rapidly in this information era, improving the transport techniques of data packets becomes a demanding task [5]. Thus, it is important to study how to improve routing protocols for packet delivery in the Internet. It is known that when the amount of packets exceeds the transport capability, a jamming transition (JT) from a free-flow state to a congested state occurs in the system [6]. The JT depends on various aspects of the system, such as network structure [7, 8], routing and queuing protocols [6, 9–18], and bandwidths of routers and optical cables [19–23]. In this paper, we focus on the JTs arising from different routing protocols. We are particularly interested in the transition types of JTs, such as continuous and discontinuous phase transitions. Even though the conventional JT in packet transport is continuous, some recently introduced models exhibit discontinuous JTs [16–19]. Thus, the goal of this paper is to uncover the differences in the mechanisms underlying the continuous and discontinuous JTs and compare the packet transport performance among the types of JTs.

To this end, we perform extensive simulations of packet transport in the Internet at the autonomous system (AS) level, for which topology information is available from the DIMES project [24]. We choose four different AS networks collected each January from 2007 to 2010 and perform simulations of packet transport on their giant components. Since we found that the behaviors of the JT on each network were similar, we carried out extensive simulations on the AS network in January 2010. The AS network is composed of nodes (ASes) with $N = 26429$ and mean degree $\langle k \rangle \simeq 6.3$. The network is scale-free, and the degree distribution follows a power law with the exponent $\gamma \simeq 2.1(1)$. With this AS network, we perform the following traffic dynamics: At each time step, every node generates a packet with rate p, which is sent toward a randomly chosen destination. During the journey, when packets arrive at the same node simultaneously, they are accumulated in the queue and forwarded one by one, following the first-in-first-out rule, to the nearest neighbor node determined by the routing protocol. We assume that the bandwidth of each node is uniform as one packet per time step regardless of the number of connections of each node. In addition, the queue size is assumed to be unlimited. Upon arriving at destinations, packets are removed from the system. We use three different routing protocols: (i) Packets are sent along the shortest path between a starting node and a destination. This protocol is referred to as the shortest path (SP) protocol [6]. (ii) Packets are sent along a globally optimal path for which the sum of the distance from a present node to the destination and the waiting times spent in the queues on the way is minimized. This protocol is referred to as the globally optimal (GO) protocol [15]. (iii) Packets are sent along a locally optimal path for which the sum of the distance from a present node to the destination and the waiting time at the nearest neighbor on the path is minimized. This protocol is referred to as the traffic-aware (TA) protocol [16]. It has been found that the order parameter of the JT behaves differently for the three protocols. For the first two protocols, the JT is continuous, while for the third protocol it is discontinuous. These protocols are represented formally as follows: Let L_i be the effective distance from node i to a target node. Then, L_i is written for the SP, GO, and TA routing protocols as follows:

$$L_i^{\rm SP} = d_i, \tag{1}$$

$$L_i^{\rm GO} = d_{\rm x} + \sum_{j\in {\rm x}} q_j(t-1), \quad \text{and} \tag{2}$$

$$L_i^{\rm TA} = h d_i + (1-h) q_i(t), \tag{3}$$

respectively, where d_i is the hopping distance between node i and the target along the shortest path. $d_{\rm x}$ is the hopping distance from node i to the target along a given path x, and $q_i(t)$ is the number of packets contained in the queue of node i at time t. h is a traffic-control parameter. It is known that as long as $0 < h < 1$, the behavior of the JT is discontinuous [16]. In our simulations, we use a fixed value of $h = 0.5$. We can classify

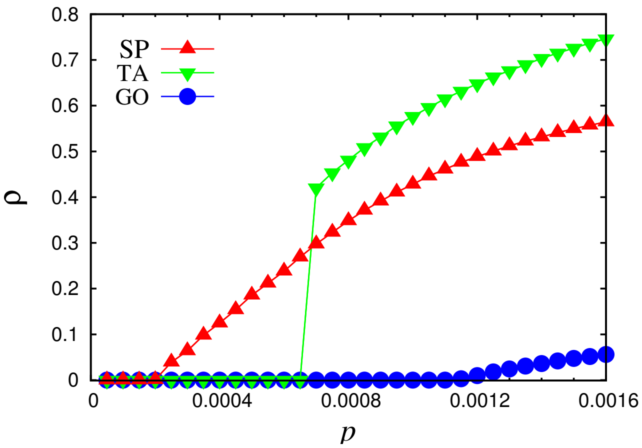

FIG. 1. (Color online) The order parameter ρ for the three routing protocols, SP ($\triangle$), TA ($\bigtriangledown$), and GO ($\bigcirc$) versus the packet generation rate p. While the protocols SP and GO exhibit continuous JTs, TA exhibits a discontinuous JT.

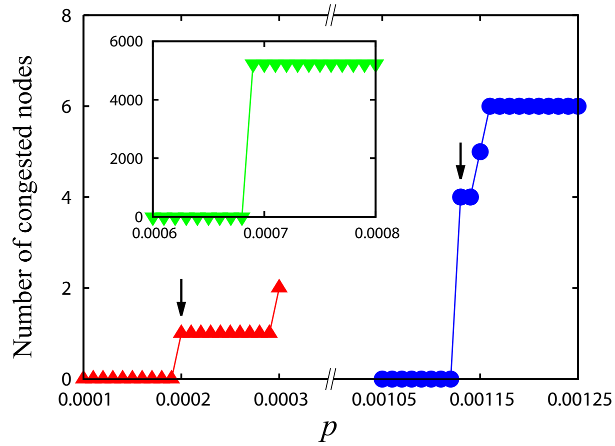

FIG. 2. (Color online) The number of congested nodes for routing protocols SP ($\triangle$) and GO ($\bigcirc$) around their critical points p_c. These numbers are small compared to the system size. Arrows indicate the JT points. Inset: The number of congested nodes for TA ($\bigtriangledown$). The number of congested nodes ($\simeq 5232$) is comparable to the system size, $N = 26429$. The threshold is taken as $q_{\rm jam} = 35$.

these protocols into two types: static and dynamic. The SP protocol belongs to the former, and GO and TA belong to the latter. However, the behavior of the JT does not follow this classification: the JTs for the first two protocols are continuous, while the JT for the third protocol is discontinuous. We perform simulations up to 10^5 time steps using the parallel updating method.

We introduce the order parameter ρ for the JT, defined as

$$\rho \equiv \lim_{t\to\infty} \frac{\langle A(t+\Delta t) - A(t)\rangle}{Np\Delta t}, \tag{4}$$

where $A(t)$ is the total number of packets in the network at time t and $\langle\cdots\rangle$ means the average over time window Δt. If the number of created packets balances the number of arrived packets on average, ρ is zero. This state is referred to as a free-flow state. However, if the number of created packets is larger than the number of arrived packets, $A(t)$ increases in time. Hence, $0 < \rho \le 1$, and this state is defined as a congested state. There is a critical value p_c across which the jamming transition occurs from the free-flow to the congested state.

We measure the order parameter ρ as a function of the packet generation rate p for the three routing protocols. Fig. 1 shows that protocols SP and GO lead to continuous JTs as p increases, while TA leads to a discontinuous JT. This result confirms the results in Refs. [6, 15, 16]. The height of the jump in the order parameter after the onset of JT indicates the ratio of the number of jammed packets to the number of created packets per time step. Thus, the non-zero value of the jump in ρ for the TA case in Fig. 1 implies that a large fraction of packets are congested at the onset of the discontinuous JT, while a small fraction of packets are jammed when the continuous JT occurs for the SP and GO cases. The JT points of the three protocols are ordered as $p_c^{\rm GO} \simeq 0.00113 > p_c^{\rm TA} \simeq 0.00069 > p_c^{\rm SP} \simeq 0.00020$. This means that the JT can be sustained up to the largest p under the GO protocol. However, the GO protocol requires the most computational power to find the optimal path, which is quite complex.

We can also view JTs in a different way. Though ρ can give information about the overall balance between packet creations and annihilations, it does not give any information about the spatial distribution of congestions in the system. To resolve this problem, we measure the number of congested nodes as a function of p. The state of a node can be defined as follows: If a node is in the free-flow state (congested state), the queue length of a node remains stationary (increases with time) with some fluctuations. To identify congested nodes, we use a threshold $q_{\rm jam}$ such that if the queue length of a node exceeds the threshold in the final stage of the simulation, that node is regarded as congested. By taking an appropriate value of $q_{\rm jam}$, we identify the state of nodes easily with negligible artificial errors. We take $q_{\rm jam} = 35$ in this study and we confirm that this actually works by estimating the growing trend of the queue length of those nodes. As shown in Fig. 2, while the SP and GO protocols generate a few congested nodes at their JT points, a large fraction (about 20%) of the total nodes in the system become congested for the TA case. This result indicates that a continuous (discontinuous) JT appears when the congestion happens locally (globally). Since a large number of nodes break down after the discontinuous JT, many packets passing through such congested nodes become jammed. This explains why the large jump in ρ for the TA protocol occurs. It is also notable that the two dynamic routing protocols, GO and TA, exhibit different congestion spreading behaviors. Hence, we can conclude that not all dynamic routing protocols tend to spread out

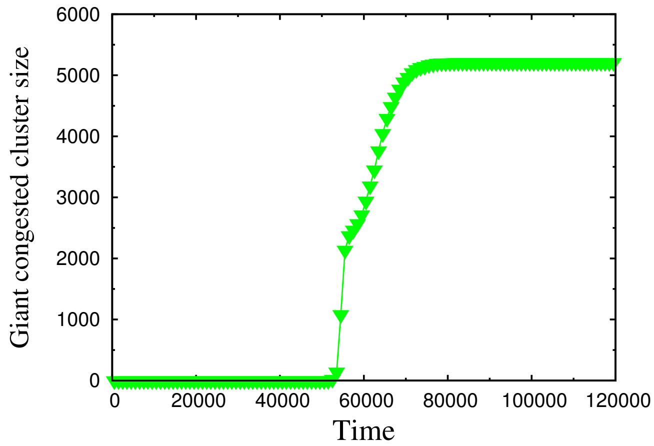

FIG. 3. (Color online) Size of the giant congested cluster versus time at the JT point for the TA protocol. At the onset of the JT, the size of the giant congested cluster grows dramatically with time.

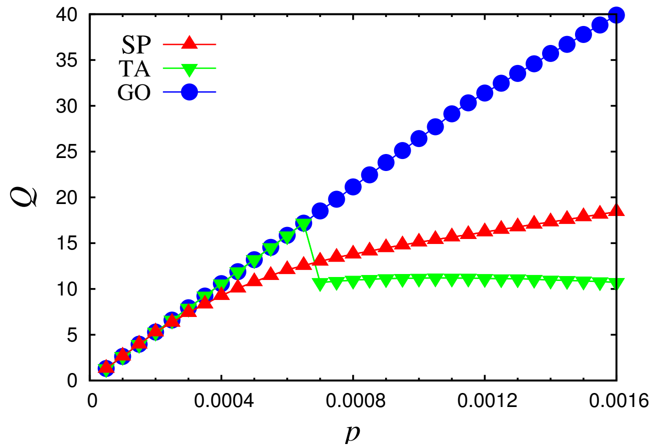

FIG. 4. (Color online) Plot of the transportation efficiency Q of the network for the three routing protocols as a function of packet generation rate p. All protocols exhibit similar performance in the region of small p. Across the JT points, Q behaves differently depending on the routing protocols.

local congestions to other nodes.

To better understand the mechanisms underlying the distinct types of JTs, we study in detail the evolution of congestions for each protocol. First, for the SP case, the mechanism is rather simple: only a node with the largest betweenness centrality (BC) [25] becomes congested when p reaches p_c [7]. There is no cascading behavior from this congested node to other nodes. The congestion behavior of a certain node is independent of those of other nodes and is determined only by the BC distribution of an underlying network. As p increases beyond p_c, the nodes with the next largest BC become congested in order. Next, for the GO case, we find that congested nodes do not coincide with the nodes having the largest BCs but rather are the nodes on the bridges between large sub-clusters. To identify such nodes, we define a connectedness centrality of node i as

$$c_i \equiv \frac{G_0 - G_i}{G_0}, \tag{5}$$

where G_0 is the giant component size of the original AS network and G_i is the giant component size of the network after the removal of node i. Thus, c_i represents a fraction of the nodes from which packets should traverse node i in order to reach other regions of the system. Therefore, nodes having large c_i are inevitable bottlenecks for any routing protocol. We confirm that the six congested nodes after the onset of JT for the GO protocol have the six largest c_i values. It is notable that the number of congested nodes remains unchanged even when p increases beyond p_c, as shown in Fig. 2. This implies that the GO protocol is indeed optimal since it delays the congestions as long as possible for all nodes except a few unavoidable bottleneck nodes.

For the TA protocol case, numerous congested nodes are created at the JT point because the TA protocol cannot guide packets to optimal paths owing to a lack of global traffic information. Since many nodes have long queues near p_c, the second term in Eq. (3) becomes dominant, and the TA protocol cannot consider topological information properly. As a result, packets do not get closer to their destinations and they become trapped in some regions. Consequently, congestions initially triggered from a few nodes can be spread to their neighboring nodes successively under the guidance of the TA protocol. To monitor the cascading behavior of congestions, we identify the largest cluster composed of congested nodes only and measure its size as a function of time (see Fig. 3). We find that the cluster grows dramatically in a short time interval, then it increases gradually and eventually saturates. This indicates that the local congestion triggered from a few nodes spreads out rapidly and forms a global congestion in a short time. Owing to this spreading of congestions, the order parameter ρ and the number of congested nodes grow discontinuously at the JT point.

Next we investigate the transportation efficiency Q:

$$Q \equiv D(T)/T, \tag{6}$$

where $D(T)$ is the number of packets arriving at their targets up to the simulation time T. Fig. 4 shows that Q has a maximum at p_c for the discontinuous JT, while Q increases monotonically even after p_c for the continuous JT. This indicates that the system achieves its best performance at p_c for the discontinuous case, but it does not for the continuous cases. If the discontinuous JT occurs, a large fraction of the nodes in the system lose their functions, and packets passing through these congested nodes are trapped in them. Consequently, they cannot reach their destinations. However, for the continuous JT, most parts of the system, except a few congested nodes, remain in the free-flow state, so that most packets still flow to their targets without severe obstruction from jamming. Therefore, maximal system transportation ef-

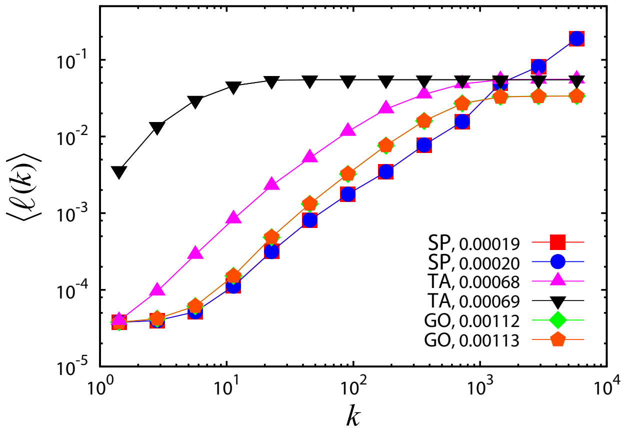

FIG. 5. (Color online) Average load $\langle \ell(k) \rangle$ of the nodes with degree k normalized by the total number of created packets during simulations for the three routing protocols, before and after their JTs; SP protocol before (□) and after (◯) p_c, TA protocol before (△) and after (▽) p_c, GO protocol before (◇) and after (⬠) p_c.

ficiency occurring at p_c, due to a massive breakdown in the system, is a reliable indicator of a discontinuous JT.

The pattern of localized (globalized) congestions for the SP and GO protocols (TA protocol) can also be found in the relation between load and degree. The load of a node is the number of packets passing through the node during the simulation [25]. We measure the average load $\langle \ell(k) \rangle$ of the nodes with degree k normalized by the total number of created packets during simulations as a function of degree k; the average is taken over the nodes with the same degree. Fig. 5 shows that for the TA protocol, there is an abrupt change in the behavior of $\langle \ell(k) \rangle$ after the discontinuous JT takes place. $\langle \ell(k) \rangle$ is rather flat for the large k region for TA after the JT. This indicates that for the TA protocol, the congestions spread out in a wide region of nodes with relatively small degree, while the congestions are localized in a few nodes for the SP and GO protocols.

In summary, we have studied jamming transitions (JTs) under three routing protocols, guiding packets to travel (i) along the shortest path, (ii) along the optimal path, and (iii) along the traffic-aware path. We found that a large fraction of nodes became congested for protocol (iii), which led to a discontinuous JT; otherwise, the JT was continuous. Protocol (iii) suppresses the accumulation of packets in a single queue and spreads them out to other nodes. As a result, the number of congested nodes increases, but with medium queue length. This mechanism is closely analogous to that of the explosive percolation transition, recently the subject of intensive study, in which the formation of the giant cluster is suppressed but medium-size clusters are produced abundantly [26–28]. In addition, we expect that models that account for a rejection rule or a finite queue would also cause this cascading of congestions in very similar ways, and thus they would lead to a discontinuous JT [17–19]. We conclude that the mechanism of inducing the spread of congestions is a key factor in discontinuous JTs.

ACKNOWLEDGMENTS

This study was supported by an NRF grant awarded through the Acceleration Research Program (Grant No.2010-0015066) and the NAP of KRCF (BK).

[1] R. Albert and A.-L. Barabási, Rev. Mod. Phys. **74**, 47 (2002).
[2] S. Boccaletti, V. Latora, Y. Moreno, M. Chavez, and D.-U. Hwang, Phys. Rep. **424**, 175 (2006).
[3] A. Barrat, M. Barthélemy, and A. Vespignani, *Dynamical Processes on Complex Networks* (Cambridge Univ. Press, Cambridge, 2008).
[4] S. N. Dorogovtsev, A. V. Goltsev, and J. F. F. Mendes, Rev. Mod. Phys. **80**, 1275 (2008).
[5] R. Pastor-Satorras and A. Vespignani, *Evolution and Structure of the Internet: A Statistical Physics Approach* (Cambridge University Press, Cambridge, England, 2004).
[6] T. Ohira and R. Sawatari, Phys. Rev. E **58**, 193 (1998).
[7] R. Guimerà, A. Díaz-Guilera, F. Vega-Redondo, A. Cabrales, and A. Arenas, Phys. Rev. Lett. **89**, 248701 (2002).
[8] Z. Toroczkai and K. E. Bassler, Nature (London) **428**, 716 (2004).
[9] R. V. Solé and S. Valverde, Physica A **289**, 595 (2001).
[10] G. Yan, T. Zhou, B. Hu, Z.-Q. Fu, and B.-H. Wang, Phys. Rev. E **73**, 046108 (2006).
[11] B. Danila, Y. Yu, J. A. Marsh, and K. E. Bassler, Phys. Rev. E **74**, 046106 (2006).
[12] B. Tadić, S. Thurner, and G. J. Rodgers, Phys. Rev. E **69**, 036102 (2004).
[13] B. Tadić, G. J. Rodgers, and S. Thurner, Int. J. Bifur. Chaos **17**, 2363 (2007).
[14] S. Sreenivasan, R. Cohen, E. López, Z. Toroczkai, and H. E. Stanley, Phys. Rev. E **75**, 036105 (2007).
[15] K. Kim, B. Kahng, and D. Kim, EPL **86**, 58002 (2009).
[16] P. Echenique, J. Gómez-Gardeñes, and Y. Moreno, Europhys. Lett. **71**, 325 (2005).
[17] D. De Martino, L. Dall'Asta, G. Bianconi, and M. Marsili, Phys. Rev. E **79**, 015101(R) (2009).
[18] S. Meloni and J. Gómez-Gardeñes, Phys. Rev. E **82**, 056105 (2010).
[19] Z.-X. Wu, W.-X. Wang, and K.-H. Yeung, New J. Phys. **10**, 023025 (2008).
[20] L. Zhao, Y.-C. Lai, K. Park, and N. Ye, Phys. Rev. E **71**, 026125 (2005).
[21] M.-B. Hu, W.-X. Wang, R. Jiang, Q.-S. Wu, and Y.-H. Wu, EPL **79**, 14003 (2007).
[22] X. Gong, L. Kun, and C.-H. Lai, EPL **83**, 28001 (2008).

[23] B. Danila, Y. D. Sun, and K. E. Bassler, Phys. Rev. E **80**, 066116 (2009).
[24] Y. Shavitt and E. Shir, ACM SIGCOMM Comput. Commun. Rev. **35**, 71 (2005); http://www.netdimes.org.
[25] K.-I. Goh, B. Kahng, and D. Kim, Phys. Rev. Lett. **87**, 278701 (2001).
[26] D. Achlioptas, R. M. D'Souza, and J. Spencer, Science **323**, 1453 (2009).
[27] Y. S. Cho, J. S. Kim, J. Park, B. Kahng, and D. Kim, Phys. Rev. Lett. **103**, 135702 (2009).
[28] Y. S. Cho, B. Kahng, and D. Kim, Phys. Rev. E **81**, 030103(R) (2010).